

# A spatial template for the shape of tuning curves in the mammalian cochlea<sup>a)</sup>

Eric L. LePage<sup>b)</sup>

Boston University, Departments of Otolaryngology and Biomedical Engineering, 80 E. Concord Street, R903, Boston, Massachusetts 02118

(Received 13 March 1986; accepted for publication 7 January 1987)

The shape of the tuning curve of primary auditory neurons of four mammals is characterized using a simple exponential model. The regression analysis formalizes a distinction between the characteristic frequency of a neuron and its "nominal" characteristic frequency in cases of temporary threshold loss in high-frequency neurons. Second, the model offers a stronger quality test for sharpness of tuning than the  $Q_{10\text{ dB}}$  since it takes into account the threshold of the neuron at its characteristic frequency and its "characteristic place" of origin along the cochlear partition. Third, the model reveals that the low-frequency side of the tip segment of the tuning curve is bounded by a constraint or template which is most simply expressed in spatial terms. The template describes the basal-side boundary of an "excitatory region" whose length along the cochlear partition is proportional to the square root of the sound pressure. Tuning curve variability arises because biological dependencies influence the basic template. A "spatial-filter" hypothesis is developed and its generality is discussed, particularly in regard to the case of the acoustic "fovea" of the horseshoe bat. Finally, the possibility is discussed that the template possesses a simple physiological correlate in the form of a spatially localized region marked by a "dc" shift of the mean position of the basilar membrane which sets the sensitivity of the tuning mechanism [E. L. LePage, *J. Acoust. Soc. Am.* **82**, 139–154 (1987)].

PACS numbers: 43.63.Kz

## INTRODUCTION

Experiments on the effects of noise trauma on the tuning characteristics of single neurons by Kiang *et al.* (1976), Robertson and Johnstone (1979), Robertson *et al.* (1980), and Liberman (1982) show that acoustic trauma or other localized damage can destroy the unique, one-to-one correspondence between the characteristic frequency (CF) and the place of origin of neurons. Neurons with reduced sensitivity are most sensitive at frequencies less than the CF associated with their point of origin. Using horseradish peroxidase (HRP) tracer studies, Liberman (1982) and Robertson (1984) have been able to assign expected frequencies to neurons on the basis of their point of origin along the cochlear partition and have found that the actual values of "best frequency" (BF) or "nominal CF" may differ significantly from the "expected CF" for the point of origin. Now there is ambiguity about whether the term "characteristic frequency" refers to a frequency corresponding to a particular *place*, or to the frequency of actual maximum sensitivity.

The behavior of the tuning curve under conditions of reduced sensitivity is an integral aspect of the tuning process in mammals. Hence, any model of the "second-filter" mechanism (Evans and Wilson, 1973), must account for changes in the shape of the tuning curve, as well as the basic shape itself. As shown by Evans (1974), disturbances produced by

anoxia, cyanide, and the diuretic furosemide result in a lowering of the BF. Sewell (1984) has also shown that injection of furosemide produces a reversible reduction in sensitivity and shift in the CF of neurons. The CF of low-frequency neurons shifts upward with decrease in the endocochlear potential, while that for high-frequency neurons shifts downward. The mechanism for these shifts is unclear.

Some evidence for sharp tuning associated with high thresholds exists in the literature (Dallos and Harris, 1978; Evans and Wilson, 1975), but most studies suggest that an inverse relation exists between the neuron's threshold at its CF and the frequency selectivity at the tip. Robertson and Manley (1974) showed that higher values of  $Q_{10\text{ dB}}$  (e.g., 4 or 5) are correlated with lower thresholds (less than 20 dB SPL). This empirical relation suggests that if the threshold of a primary afferent neuron could be extrapolated downward to very low sound levels, a limiting condition might be encountered and the BF might converge toward an asymptote of fixed frequency. This would be the CF of that place. Cody and Johnstone (1980) clearly demonstrated such a trend for a single neuron. They recorded the tuning curve intermittently during a 127-min exposure to a loud tone. The neuron exhibited a progressive decline in both its sensitivity and its sharpness of tuning. Their data, reproduced in Fig. 1(a), suggests quite strongly that as the threshold rose, the BF diverged from the CF along the dashed line. These data also illustrate that despite threshold loss, the basic shape or template of the tuning curve appears to be preserved.

Figure 1(b) illustrates the mathematical model that is described below. The two "sides" of the threshold tuning curve may be conceived as being determined semi-independently.

<sup>a)</sup> An earlier version of this paper was presented at the symposium "Mechanics of Hearing" in Delft, The Netherlands, July 1983.

<sup>b)</sup> Present address: Department of Physiology, The University of Western Australia, Nedlands, W. A. 6009, Australia.

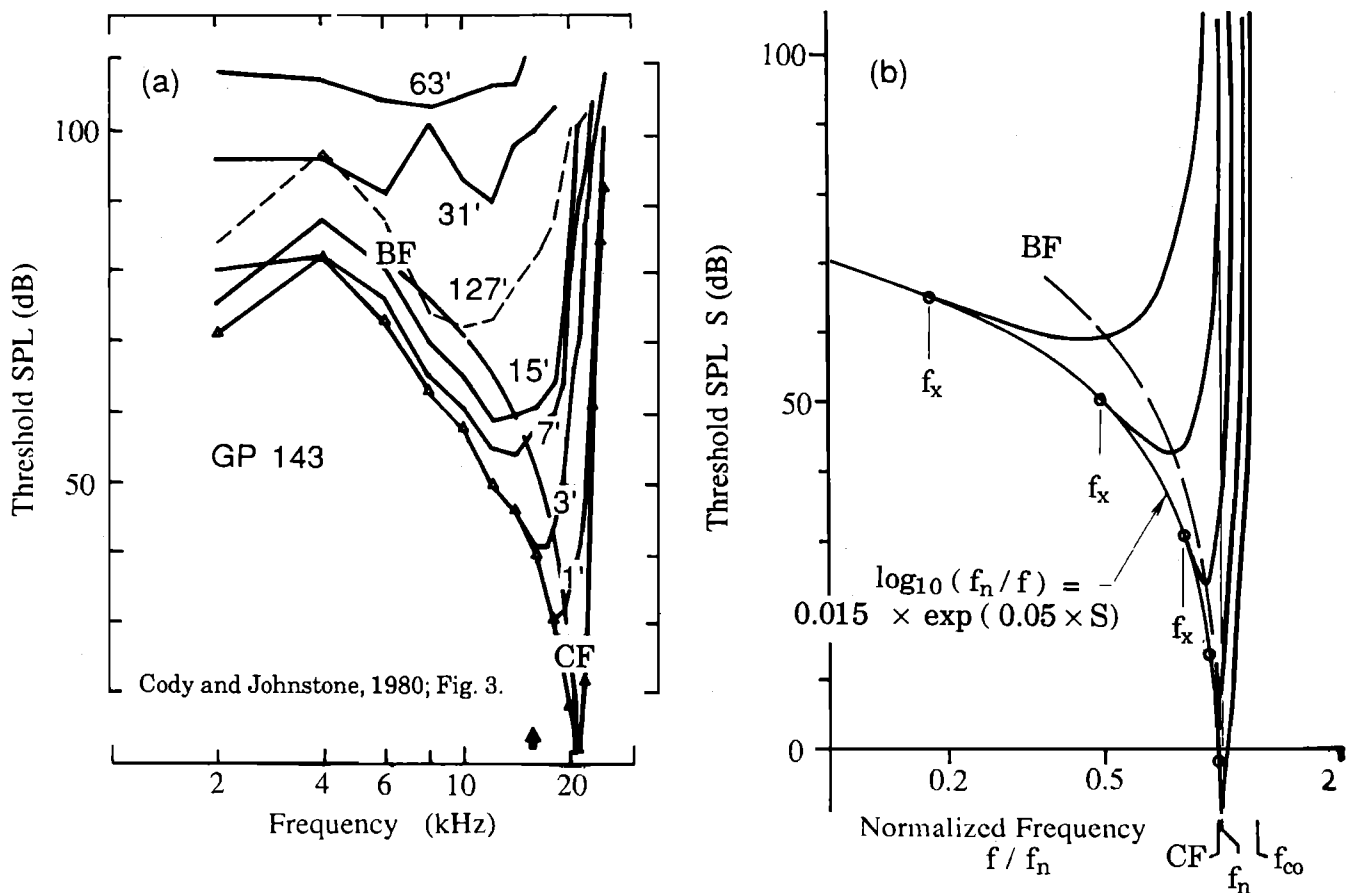


FIG. 1. (a) Response of a single guinea pig spiral ganglion cell over a 127-min period in which the cochlea was exposed to a 16-kHz tone at 100 dB SPL. The tone was interrupted at periodic intervals, long enough to obtain the fiber threshold response. The tuning curve displays a progressive loss of sensitivity and decrease in the "nominal" CF from its original CF of 21 kHz. The characteristic shape of the tuning curve appears to be retained despite loss of sensitivity and change in CF (reproduced with permission of A. R. Cody). (b) Schematic diagram of the model. The low- and high-frequency sides of the tuning curve are treated separately. The dividing line for any tuning curve is not at the CF but at a frequency  $f_x$  on the low-frequency side, at which a point of inflection occurs. For frequencies below  $f_x$  the tuning curve generally appears to be constrained by a curve which asymptotes to a "limit" or "natural" frequency  $f_n$ . Above  $f_x$  the tuning curve departs from the constraint and exhibits a frequency of maximal sensitivity (BF) and the cutoff at frequency  $f_{co}$ . The constraint is a simple exponential in which sound intensity is the independent variable. The exponential asymptotes to a value of unity—the normalized limit frequency corresponding to the place of origin of the neuron. The best frequency (BF) also asymptotes along a similar exponential curve to the same asymptote. The characteristic frequency of the nerve fiber is viewed as the highest value of the BF imposed by some biological limit on how far  $f_x$  is "driven" down the curve toward  $f_n$ . The model does not define the high-frequency slope of the curve and regards the cutoff frequency  $f_{co}$  as being dependent on the value of  $f_x$ . The two coefficients  $\alpha$  and  $\beta$  have physiological significance. Here,  $\alpha$  is effectively the gradient of the frequency-place map for the species, while  $\beta$  is remarkably constant across species.

dently and not by a single resonant process acting upon a localized section of the basilar membrane. Each curve is divided into two frequency regions, one above and one below a point of inflection ( $f_x$ ) on the low-frequency side of BF. The point lies within 10 dB of the tip threshold. For frequencies below  $f_x$ , the tuning curve tends to adhere closely to the model. This range is the half-octave below CF, within which an active process seems to be in action (Neely and Kim, 1983). [Of course, this description is simplified. The curves with high thresholds shown in Fig. 1(a) appear to have suffered an additional elevation of thresholds which is not frequency dependent, such as due to dendritic swelling (Robertson, 1983, Fig. 7).] Each tuning curve departs from the model at its particular  $f_x$  and reaches its maximum sensitivity at its BF. Beyond this, the tuning curves rise steeply and tend toward a limit at a cutoff frequency  $f_{co}$ . The BFs follow a second curve which seems to approach to the same limit as the  $f_x$  curve approaches a "limit" or "natural" frequency  $f_n$ .

The two asymptotic curves appear to be related and special attention will be devoted to characterizing the low-frequency portion of the neural tuning curve.

## I. PROCEDURE

Published and unpublished data were taken from guinea pig, cat, squirrel monkey, and mongolian gerbil in order to describe the low-frequency branch of the tuning curve with a simple mathematical model. From these species, low-threshold tuning curves have been selected for minimal disparity between the BF of each neuron and its expected CF.

These data were digitized by storing pairs of coordinates for frequency and threshold level (dB) for whole tuning curves. As shown in Fig. 2, the "tail" section of the curve was omitted from the curve fitting procedure, as was the high-frequency branch of the curve above the CF. Frequently, a curve is irregular above about 75-dB stimulus level and does

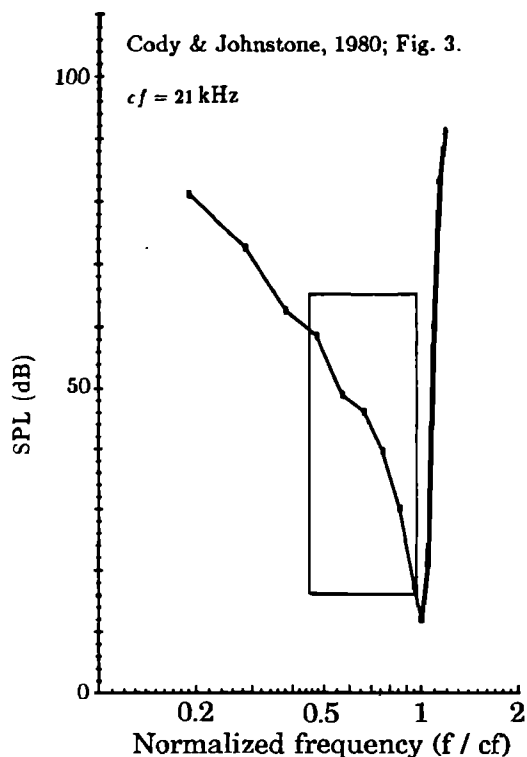


FIG. 2. The method of interactive selection of points for the nonlinear regression. The tuning curves are first normalized by dividing the frequencies by the measured value of the characteristic frequency. Points on the tuning curve inside the box are fitted for minimum least squares. Points for frequencies above  $f_x$  and below the "active" region are eliminated. Similarly, points in the "tail" region above ca. 70 dB are also eliminated.

not conform to the trend under study and therefore curve fitting was restricted to lower levels. A salient feature of the low-frequency branch is the point of inflection marking the point of departure of the tuning curve from the asymptotic trend as the tip is approached. Any points beyond that departure were also eliminated from the curve fitting procedure. The remaining points were enclosed in a box (see Figs. 2–6) and only those were used for the analysis.

The curve fitting procedure itself is an iterative least-square analysis for nonlinear functions provided by Wolberg (1967). The objective was that the model should show an asymptotic trend of the curve to the CF as the sound level (dB) was reduced. A variety of nonlinear functions were tested against the neural data and a simple exponential function clearly provided the best fit. In order to use an exponential function in this way, the frequencies were normalized to unity at the CF, and the sound level (dB) was deliberately chosen as the *independent* variable, with uniform weighting of the errors over the decibel range within the box. Hence, the quantity being minimized was the sum of the squares of the differences between the function and the logarithm of the normalized frequency of the threshold test tone.

The equation chosen for the fit was

$$\log_{10}(cf/f) = \alpha e^{\beta S}, \quad (1)$$

where  $cf$  is the characteristic frequency,  $f$  is the frequency of the test tone at threshold,  $S$  is the threshold sound-pressure level, and  $\alpha$  and  $\beta$  are the fit parameters to be determined. (The left-hand side of the equation is therefore 0.3010 times

the octave separation of  $f$  from the  $cf$ .) The procedure provides the s.d. of both parameters, the limits of which are preset at the beginning. The accuracy of the fit was further judged by computing, for both coordinates, the root-mean-square (rms) errors between the derived function and each point for all points in the box. For comparison with other methods recently used for fitting tuning curves, the mean dB error for each point was also computed. For example, Allen (1983) permitted an error up to 8 dB.

## II. RESULTS

The first example of the results for guinea pig is shown in Fig. 3. The left half of Fig. 3(a) shows the lowest tuning curve of Fig. 1 redrawn with the six consecutive points selected for the fit. The resulting curve of best fit is shown in the right half of Fig. 3(a), giving fairly typical values of 0.018 for  $\alpha$  and 0.050 for  $\beta$ . The respective s.d.'s were 0.0044 and 0.0045. The rms error for  $\log_{10}(cf/f)$  is 0.017 or 0.056 oct for all the points in the box; the rms error for the intensity is 2 dB and the mean error is again 0.5 dB for all points. Figure 3(b)–(d) shows the threshold tuning curves of other high-frequency neurons for guinea pig. Figure 3(b) shows a fit for eight nerve fibers which had been normalized in order to produce a mean tuning curve (Cody and Johnstone, 1980, Fig. 4). Figure 3(c) shows the mean tuning curve for eight different nerve fibers from Robertson (unpublished figure), while Fig. 3(d) shows a 28-kHz curve from guinea pig eighth nerve (Alder, 1978). In each case it may be seen that the curve fit is remarkably good, with the maximum rms errors being of the order of 1/30 oct and ca. 2 dB, with a mean error often much less than 1 dB.

The second set of data for cat is derived from Liberman and Kiang (1978) for four records, all from one animal. Examples of curve fits for best frequencies of 0.9 and 15.8 kHz are shown, respectively, in Fig. 4(a) and (b). In each case, the rms errors are 1/19 and 1/43 oct, while the rms dB errors are 2.7 and 2.0. The mean errors are less than 1 dB.

The third set of data shown in Fig. 5 is for mongolian gerbil (Schmiedt *et al.*, 1980) and represents ten neurons at 5.3 kHz. Again, the errors are small.<sup>1</sup>

The last set of results were derived from single-neuron recordings from squirrel monkey (Geisler *et al.*, 1974, Fig. 2). The authors specifically address the question of the shape of the tuning curve. Figure 6(a) and (b) shows two sets of original data replotted for estimated threshold rate levels above the spontaneous rate. Both sets of data show that the gradient of the low-frequency branch is steeper, as reflected in the smaller values of  $\alpha$ . It may be seen that the fit of each of these curves is remarkable, with rms errors in Fig. 6(a) of as little as 1/96 oct and 1.4 dB, and mean dB error of as little as 0.1 dB.

Figure 7 shows, by way of illustration of the model, the independent effects of variation of  $\alpha$  and  $\beta$ . In Fig. 7(a), a family of curves for a typical fixed value of  $\alpha$  is represented, while  $\beta$  is varied, showing the differing rates of growth of departure of the threshold condition from the CF with sound level. Figure 7(b) shows, for one typical value of  $\beta$ , the linear scaling effect of  $\alpha$  on the separation from the CF, reflecting  $\alpha$ 's relationship to the gradient of the frequency-place map.

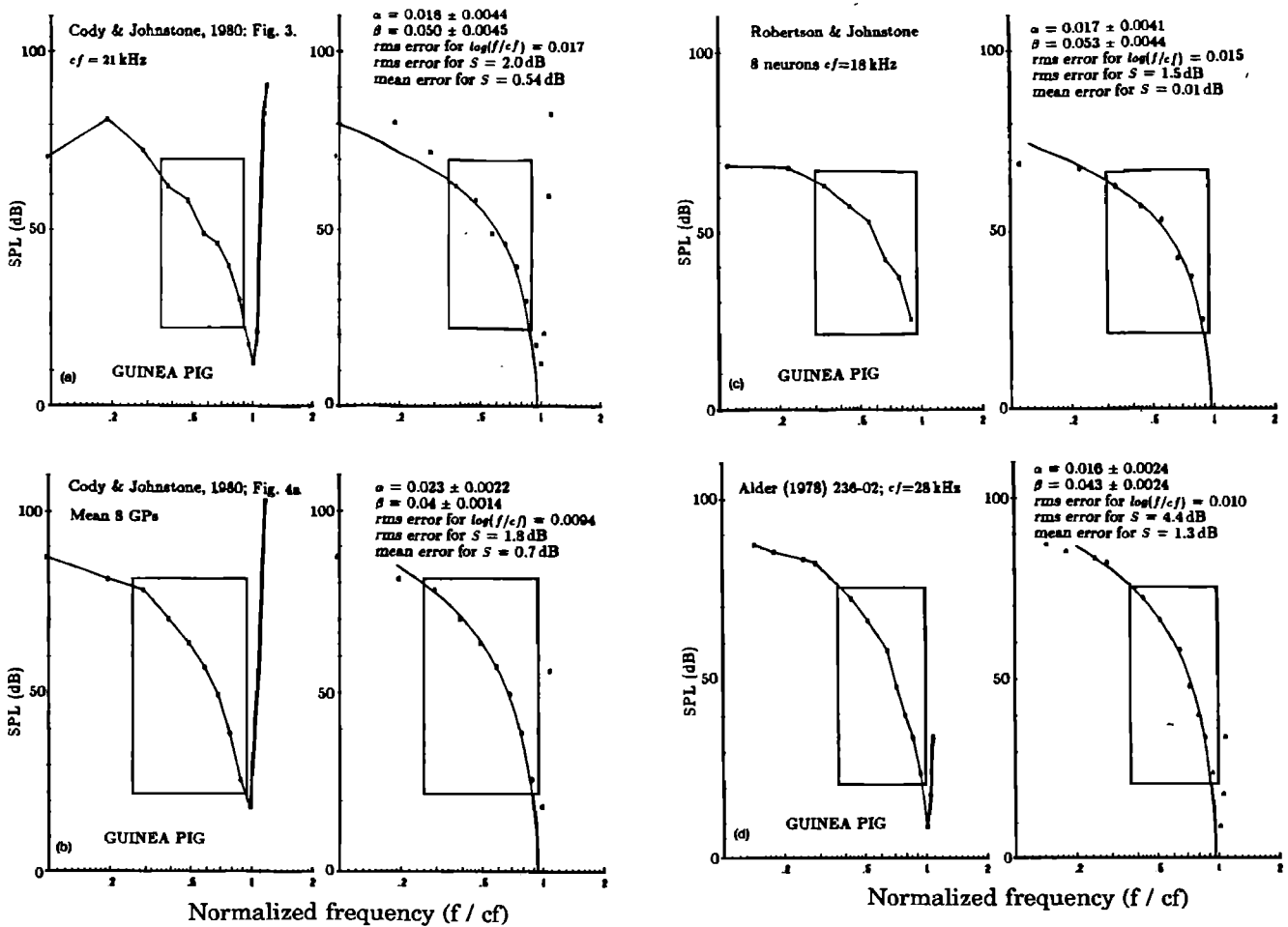


FIG. 3. (a)–(d) Regression analyses for a selection of curves for guinea pig. In each pair of panels the points of the same tuning curve are plotted identically on the two sets of axes. On the left side they are joined as for plotting the complete tuning curve as presented in the literature. In the right panel, the line of best fit is plotted through the points inside the box. The CF, if applicable, is shown below the source in the left panel. The values of  $\alpha$  and  $\beta$ , together with the given errors for the determination, are shown in the right panel. The tolerances shown for  $\alpha$  and  $\beta$  are standard deviations. In the lower two panels are averaged curves for guinea pig. [(a) and (b) reproduced with permission of A. R. Cody.] (c) Tuning curves for guinea pig showing another set of average values for the tuning curve (courtesy of D. Robertson). (d) The lower two panels show the result for a 28-kHz neuron from the eighth nerve (courtesy of V. Alder, 1978).

It is instructive to consider the range of values obtained for the fit parameters  $\alpha$  and  $\beta$ . These are plotted in Fig. 8 for the sample of curves used. In the figure P stands for guinea pig, Q for squirrel monkey, M for mongolian gerbil, and C for cat. Figure 8 suggests that  $\beta$  clusters around a value of 0.04–0.05, while the absolute value of  $\alpha$  varies from values ca. 0.004–0.07. There is a slight suggestion of correlation of  $\alpha$  and  $\beta$  in that slightly higher values of  $\beta$  may occur in species exhibiting lower values of  $\alpha$ .

To look for any other possible dependencies, both  $\alpha$  and  $\beta$  were correlated against the BF and the thresholds for the single-neuron tuning curves for the pooled data from the four species. This is shown in Fig. 9. It would appear that  $\beta$  varies very little with species, BF, and unit threshold. On the other hand, the magnitude of  $\alpha$  is strongly species dependent for BFs above 5 kHz. The squirrel monkeys as a class exhibit the lowest values (0.004), followed by guinea pig ( $< 0.02$ ), cat (0.02), and the pooled results for gerbil (0.055). The four panels show no other special interdependencies, except for a suggestion that the values of  $\alpha$  may vary with position along the basilar membrane. The three results for cat for

higher values of  $\alpha$  were derived from very low-frequency neurons; this is consistent with the results of Kim and Molnar (1979) and Liberman (1982), which show a compression of the frequency–place map toward the apex of cat.

Examining the data with the fitted curves in each case shows a clear cut departure of the points near the bottom of the tuning curve from the fitted curve. Figure 10 shows the result of deciding from each curve the difference in dB between the threshold at the tip and the sound level at the point of inflection. For these data the mean difference is 7 dB.

Small rms errors for empirically acceptable values of  $\alpha$  and  $\beta$  guarantees high values of the  $Q_{10\text{ dB}}$ , whereas the converse is not generally true. Increased errors in the fit of the curve may arise due to irregularities in the local frequency–place map basal to the origin of the neuron.

### A. Spatial interpretation of model

It is remarkable that the low-frequency side of the neural threshold curve can be so consistently and accurately

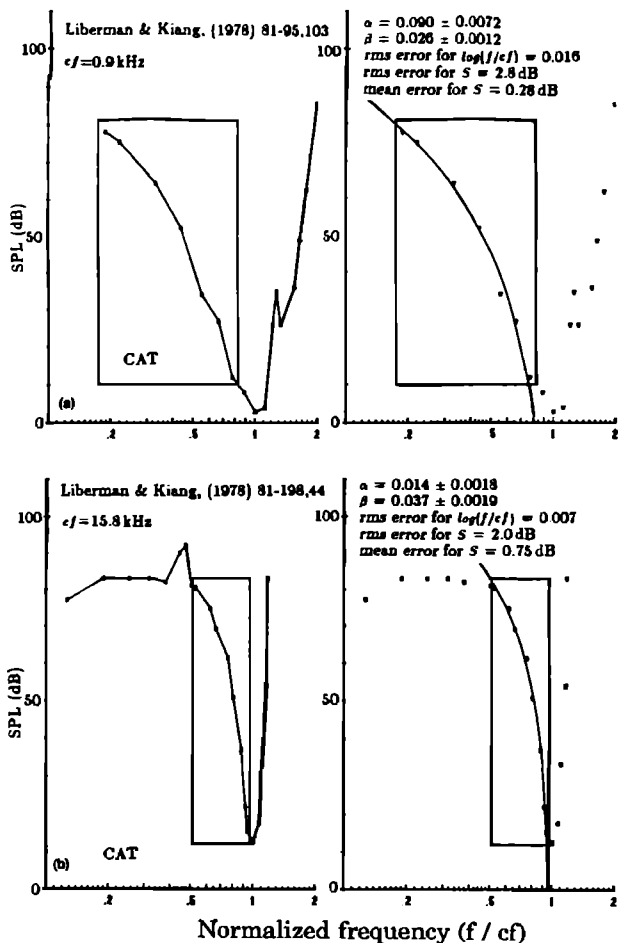


FIG. 4. (a) and (b) Upper and lower pairs of panels are from Liberman and Kiang (1978) for cat. While low-frequency neurons tend to show a shift of CF upward with loss of threshold, remarkably, 0.9-kHz CF neurons show conformance with the model. In the lower panels, a 15.8-kHz CF nerve fiber shows very small errors in the fitting of the model (reproduced by permission of M. C. Liberman).

fitted (1) by a simple exponential function with only two degrees of freedom, (2) for four species, and (3) for characteristic frequencies ranging up to 28 kHz. The relation could be even more intriguing if the range of the model extends below 1 kHz as two examples from cat suggest.

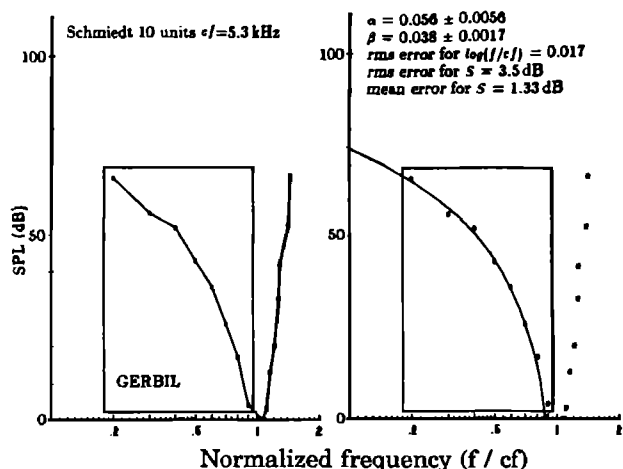


FIG. 5. Average of ten nerve fiber tuning curves for the gerbil CF of 5.3 kHz (courtesy of R. Schmiedt).

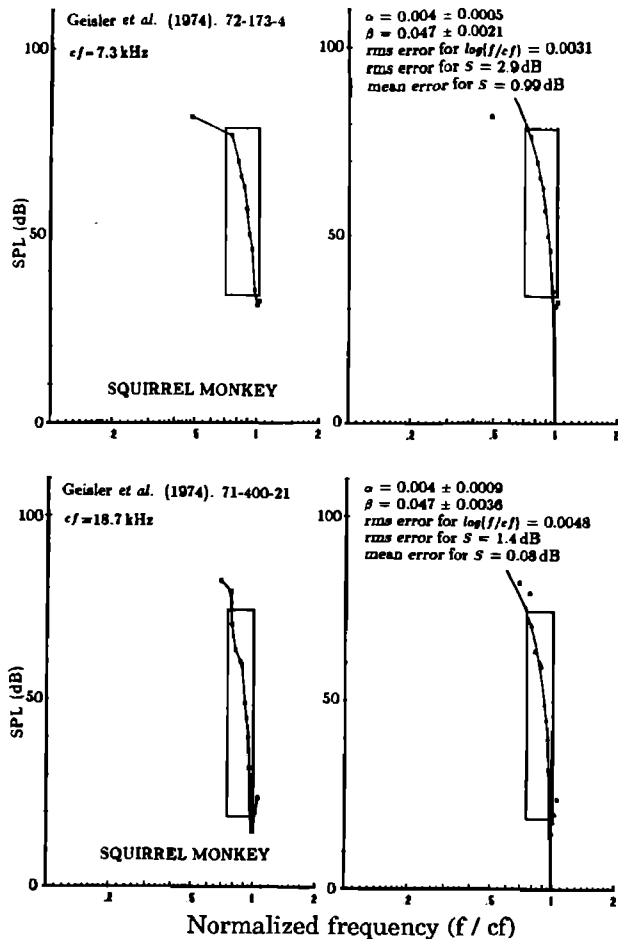


FIG. 6. Two eighth-nerve fibers from squirrel monkey. These isorate results were obtained by interpolating iso-SPL contours from Geisler *et al.* (1974, Fig. 2) (reproduced by permission of C. D. Geisler). All four examples published exhibit remarkably small errors, partly due to the interpolation procedure. The top and bottom panels are for neurons at 7.3 and 18.7 kHz.

The frequency-place map can be represented by

$$\Delta x = \gamma \log_2(cf/f), \quad (2)$$

where  $\Delta x$  is the distance (mm) of the place corresponding to  $f$  from some absolute reference place for  $cf$ , and  $\gamma$  is the gradient of the frequency-place map (mm/oct).

Substituting in (1) yields

$$\Delta x = \alpha' e^{\beta S},$$

where  $\alpha' = \gamma\alpha/0.3010$ . However, sound-pressure level is defined as

$$S = 20 \log_{10}(p/p_0) = 8.7 \ln(p/p_0),$$

where  $p$  is the sound pressure (Pa) and  $p_0$  is a reference pressure ( $20 \mu\text{Pa}$ ).

By combining,

$$\Delta x = \alpha' (p/p_0)^{8.7\beta}. \quad (3)$$

In Fig. 8 values of  $\beta$  cluster around 0.05 and extend up to 0.07. If we take a value of 0.0576, we have

$$\Delta x = \alpha' (p/p_0)^{0.5}, \quad (4)$$

or

$$\Delta x \propto \sqrt{p}. \quad (5)$$

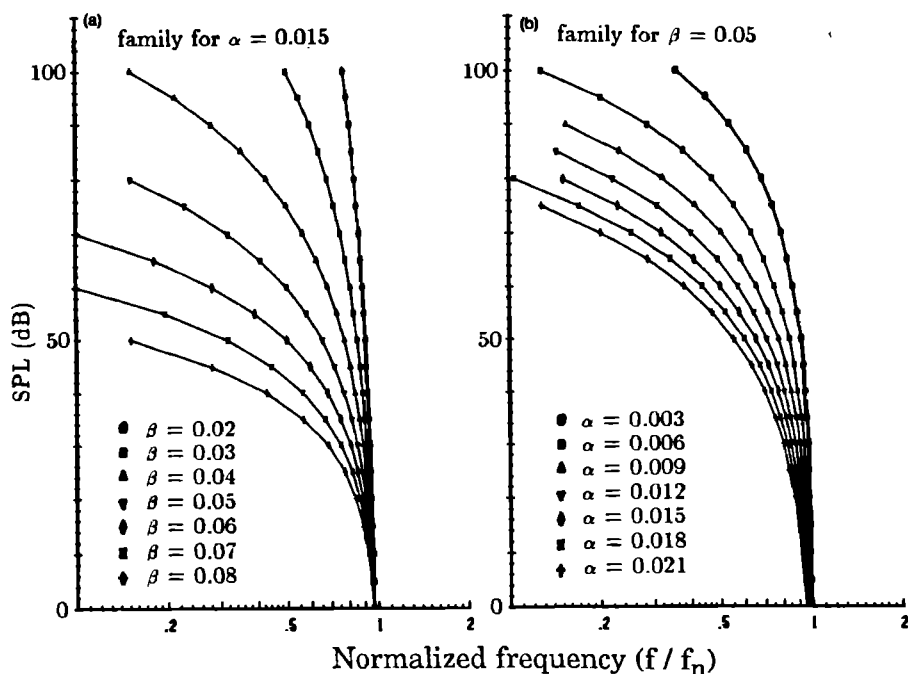


FIG. 7. Families of curves determined for the model. In (a), the curves are for fixing  $\alpha$  at a typical value of 0.015, while  $\beta$  is varied from 0.02–0.08 in steps of 0.01. (b) shows, for a typical value of  $\beta$  of 0.05, the linear scaling effect of  $\alpha$  on the normalized frequency, equivalent to scaling the gradient of the frequency–place map.

### III. DISCUSSION

The model recognizes the asymmetry of the tuning curve and, in particular, a distinction between the BF and the CF. Although temporary threshold shift causes both a change in the shape of the tuning curve and the BF of the neuron, the model illustrates that the tuning curve still retains a pointer to the original CF and therefore the place of origin of the neuron. A fine, but important point, is the concept that the CF is a special case of the BF for some limiting biological condition, but that both lie on a curve which

asymptotes to some limiting frequency  $f_n$  which is “natural” for that place. Many passive physical properties of the cochlear partition display tonotopic variation, such as the natural resonant frequency of hair cell stereocilia (Frishkopf and deRosier, 1983). The resulting behavioral frequency–place map, or the value of  $f_n$  for any “characteristic place” (CP), may be determined by a combination of these tapered parameters.

The notion of a constraint upon the tuning curve is important. First, it ties the basic shape of the tuning curve to the absolute point of origin of the neuron and predicts how the neural tuning curve will behave under conditions which indicate a loss of driving force. For example, if the endocochlear potential drops below +80 mV, such as occurs with administration of furosemide (Sewell, 1984), the value of  $f_x$  will rise along the curve described by the model. Second, the constraint places a very strong requirement upon the quality of any particular tuning curve. High values of  $Q_{10\text{ dB}}$  will aberrantly reflect sharp tuning unless the tip of the tuning curve occurs at a low, predictable sound level. Hence, the model provides a stronger quality test than the  $Q_{10\text{ dB}}$  and will serve as the basis for the empirical relation determined by Robertson and Manley (1974).

Because of sharp tuning, it has been difficult to avoid concepts and models directly involving second-order systems with highly nonlinear properties, as far as defining the shape of the tuning curve is concerned. In contrast, the final result (5) is a spatial characterization of a key feature of the neural tuning curve in mammals. For any given sound level, the equation describes precisely *where* threshold is reached. For a given frequency, a traveling wave pattern will be established with a peak at the CP. The relation says that for a pure tone of a given frequency, the particular neuron receiving threshold excitation will be at a distance, basalward from the CP, which is proportional to the square root of the sound pressure.

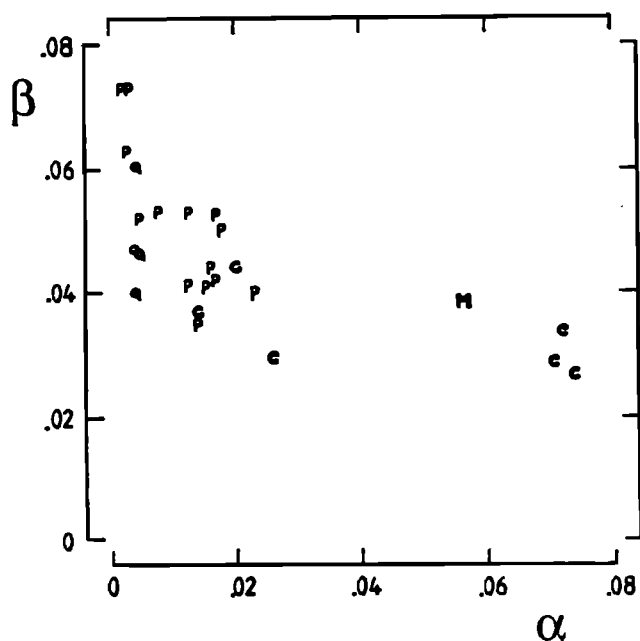


FIG. 8. Interdependence of  $\beta$  and  $\alpha$ . The sample of curves is too small to conclude interdependence. There may be, however, a suggestion that smaller values of  $\alpha$  are correlated with larger values of  $\beta$ . This does not imply mutual dependence.

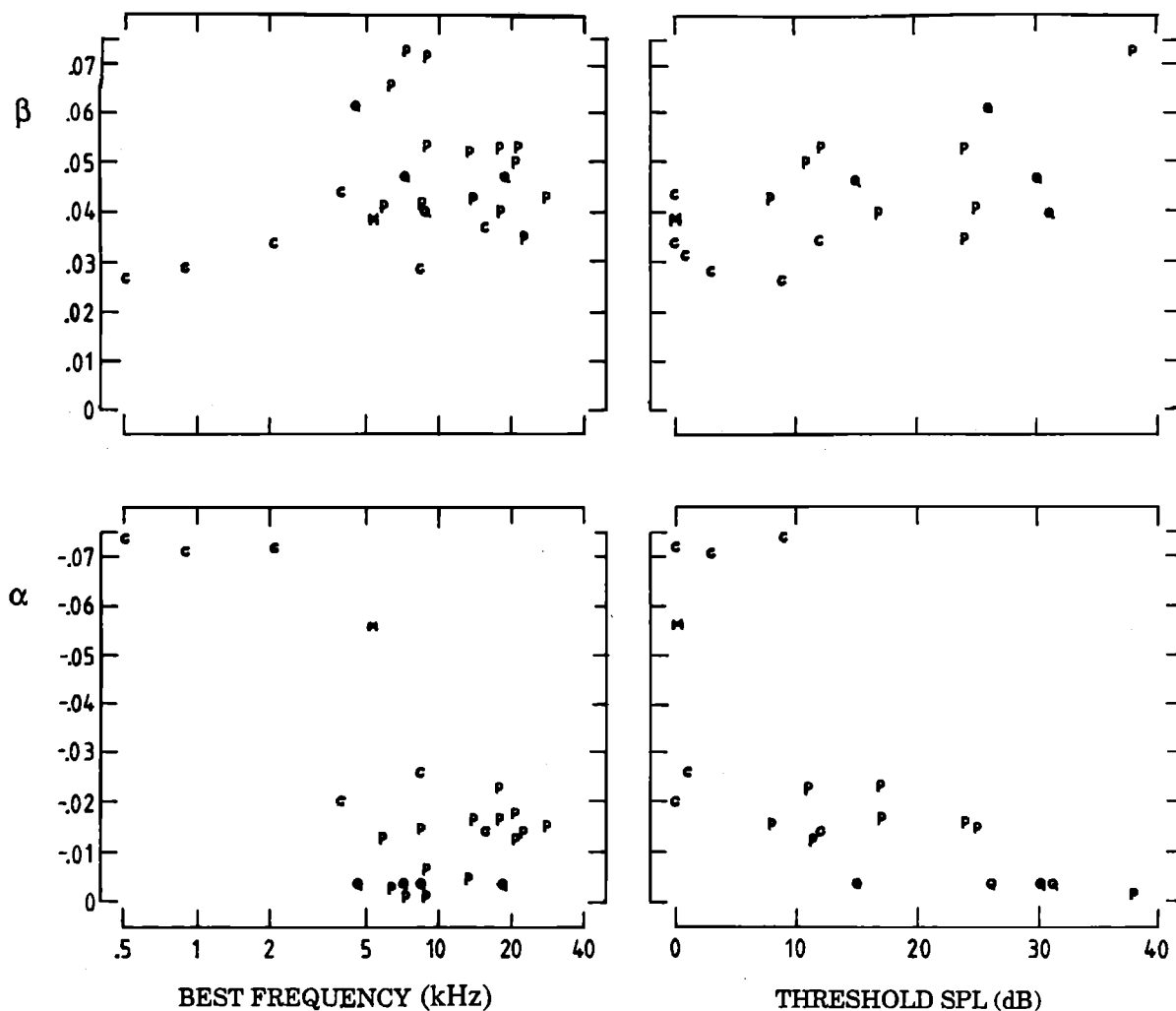


FIG. 9. Dependence of  $\alpha$  and  $\beta$  upon the "nominal" or "best" frequency and also upon the threshold at the BF. Values of  $\beta$  appear to cluster about 0.05 for all high-frequency neurons, while values of  $\alpha$  may be scaled inversely with length of the cochlea of the species. The three values for cat for very low frequencies are clearly subject to another form of dependence.

The high-frequency branch of the tuning curve, on the other hand, has a distinctly different character. The value of  $f_{co}$  appears to be fixed in relation to the value of  $f_x$ . As  $f_x$  decreases the cutoff moves to lower frequencies and decreases in slope (Liberman, 1984).

### A. Origin of the tuning curve

There is a longitudinal region of the cochlea which is in a state of "excitation" above threshold—the region associated

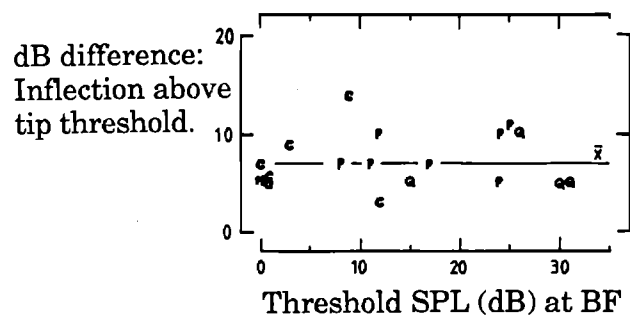


FIG. 10. The scatter plot suggests that the point of inflection at  $f_x$  occurs an average  $\bar{x}$  of 7 dB above the threshold at the CF and is independent of the sound level at the nominal CF.

with processes which have been determined to be nonlinear (Rhode, 1971; LePage and Johnstone, 1980; Sellick *et al.*, 1982), and active (Neely and Kim, 1983; deBoer, 1983a,b). The basal extent of this "excitatory region" is precisely described by Eq. (3). The basic tuning template arises because varying the frequency of the test tone causes the traveling wave envelope to slide past the detecting neuron. The sound level is adjusted by the experimenter so that for each frequency the detector receives a threshold level of excitation. Such a condition was recently proposed by Sellick *et al.* (1982) for the mechanical tuning curve. They proposed that threshold neural response corresponded to a basilar membrane velocity of 0.04 mm/s. If the mechanical tuning curve can be fitted like the neuronal tuning curves, and the new mechanical data suggest that this is possible, this suggests that in sensitive preparations 0.04-mm/s vibration occurs at a distance along the cochlear partition which is fixed by the frequency of the tone, the local gradient of the frequency-place map, and the intensity of the stimulus.

If we represent the impedance  $Z_x$  of the basilar membrane at some place  $x$  as

$$Z_x = p_x/v, \quad (6)$$

where  $v$  is a constant (0.04 mm/s) for the threshold condition and  $p_x$  is the pressure differential across the basilar membrane if  $p_x \propto p$ , this suggests that for the threshold condition

$$\Delta x \propto Z_x^{1/2}. \quad (7)$$

In other words, the last relation (7) is suggesting that it may be possible to replace the external parameter  $p$  with the internal parameter  $Z_x$  and thereby represent threshold in terms of a threshold change in the dynamic impedance of the basilar membrane.

Direct mechanical evidence has been recently provided that the basilar membrane exhibits a frequency-dependent dc component of motion in addition to the traditional traveling wave pattern (LePage and Hubbard, 1986). In a more detailed description (LePage, 1987a) two dc components, fast and slow, appear to work in tandem for frequencies that constitute the tails of tuning curves, while in the tip region, corresponding to the frequency region of interest here, the two components appear to work in opposition. Both dc components are tuned. The larger long-term dc component represents a displacement toward scala tympani. It seems likely, therefore, that the low-frequency branch of the sensitive tip segment, specified by Eq. (3), is established by the highly defined basal edge of the dc bias in the basilar membrane position. Hence, the low-frequency branch of the tip segment arises because for any stimulus frequency, the experimenter adjusts the level until the basal edge of the dc component becomes aligned with the place of origin of the neuron. It is hypothesized (LePage, 1987b) that at threshold the operating point of the outer hair cells at that place is just beginning to move into the active region of the hair cell characteristic; *that is, threshold represents a borderline condition between passive and active response of the outer hair cells.* A similar situation is likely to be established in determining the high-frequency branch of the tuning curve. As such, the shape of the two borders of the region above threshold will be unaffected by nonlinear compression. Compression will be evident in the mechanical response only at higher sound levels, for which the cells respond actively by force generation. This might explain any change in the dynamic impedance of the basilar membrane with active response of the OHCs and why the basic template of the mammalian tuning curve [see, again, Fig. 1(b)] is independent of hair cell function, and depends only upon one passive spatial parameter—the gradient of the frequency–place map. Normal response of the OHCs results in variations within that basic template. Permanent damage to micromechanical structures, on the other hand, may produce more substantial changes to the shape (Robertson *et al.*, 1978; Liberman and Dodds, 1984).

The model, therefore, represents a substantial simplification of the description of the shape of the tip segment of the tuning curve. The interpretation is that the tuning arises because the traveling wave sets up a *region of excitation* bordered on each side by regions of inhibition (LePage, 1987b). The model describes the spatial behavior of the transition from inhibition to excitation on the basal side of the traveling wave envelope. *This overall tripolar spatial pattern slides longitudinally with the traveling wave envelope as frequency is*

*varied, while its longitudinal extent expands and contracts with changes in acoustic sound level.* As the level is increased, the spatial pattern expands simultaneously toward the base and apex, but more toward the base, in proportion to the longitudinal dimensions of the traveling wave envelope. The inner hair cells respond to this steady displacement pattern as simple mechanical detectors.

## B. Effects of localized damage along the organ of Corti

A logical extension of the idea that sensitivity and sharp tuning are both dependent on the gain of the amplification mechanism is that global or local variations in the gain may produce global or local modifications in the frequency–place map. If the map becomes so distorted that it is no longer monotonic, instabilities may be expected due to reflections of the traveling wave at points of negative slope in the frequency–place map. Irregularities in tuning curves may relate to localized pathology of the organ of Corti that produce effective changes in  $\alpha'$  and consequent distortions of the map.

## C. Generality of spatial approach

The concept of spatial filtering is by no means new. Hugdins and Licklider (1951) showed a number of schemes and their potential advantages. The present analysis suggests that the cochlea may achieve its surprising filtering performance by transforming frequency and time into space and then generating simple excitation and inhibition patterns along the cochlear partition. The borders of excitation and inhibition may slide along the cochlear partition with change in sound-pressure level; the result will be akin to the spatial differentiation suggested by Hall (1977). The essential difference is that Hall was differentiating the vibratory response of the basilar membrane. LePage (1987b), however, suggests that the steady dc response of the basilar membrane is spatially tied to the traveling wave envelope. The hypothesized shifting of the “threshold-crossing” boundaries of the tripolar pattern with level is effectively a physical realization of Hall’s model. The borders of the excitatory region will be detected by the inner hair cells and transmitted through the ascending auditory pathway as regions of contrast in neural firing patterns.

The model also suggests that theoretically any degree of frequency selectivity can be attained by specializations affecting  $\alpha'$ . The spatial approach, therefore, may be equally applicable for map gradients of typically 2.5 mm/oct for guinea pig to 60 mm/oct for the acoustic “fovea” of the horseshoe bat (*Rhinolophus ferrumequinum*) (Bruns, 1976; Bruns and Schmieszek, 1980). Suga *et al.* (1976) show that this animal exhibits similarly shaped tuning curves and typical values of  $Q_{10\text{dB}}$  of 140 and high-frequency slopes of up to 3500 dB/oct. It is difficult to account for this performance by any model involving resonance of discrete, decoupled, mechanically tuned elements. Still more specialized mechanisms are apparently needed (Duifhuis and Vater, 1986). On the other hand, the spatial model naturally seems to cover the case of this bat. The thickening of the basilar membrane in this animal is viewed as a means of scaling  $\alpha'$  simply by changing  $\gamma$ . If one scales a typical value of 5.5 for the

$Q_{10\text{dB}}$  in guinea pig by the ratio 60/2.5 the requisite tuning is produced. The spatial-filter concept also allows the high-frequency slopes to be increased arbitrarily by a reduction of the amount of the hypothesized sliding shift of the excitation-inhibition boundary of the excitation region as the sound level is increased.

#### IV. SUMMARY AND CONCLUSIONS

(1) Recent experiments on the behavior of primary auditory neurons have introduced an ambiguity into the term *characteristic frequency* (CF) such that it now needs to be qualified according to the fiber's threshold. Loss of sensitivity is marked by a loss of sharpness of tuning and a shift in the CF of fibers from values expected from morphological determination of the origins of the fibers.

(2) A nonlinear model formalizes this distinction by recognizing that the behavior as a function of threshold elevation of the "best" frequency (BF) tends to follow a curve similar to the low-frequency side of the threshold tuning curve of high-frequency neurons. The analysis identifies the low-frequency side of the sensitive tip segment of low-threshold fibers within the half-octave region, where active, nonlinear behavior occurs in the cochlea.

(3) The curve of best fit to the low-frequency branch is a simple exponential in which the sound level (dB re: 20  $\mu$ Pa) is treated as the *independent* variable. Using only two coefficients,  $\alpha$  and  $\beta$ , the curve

$$\log(cf/f) = \alpha e^{\beta S}$$

(where  $cf$  is the CF of the neuron,  $f$  is the test frequency, and  $S$  is the sound-pressure level in dB for threshold excitation) yields consistent values for  $\alpha$  and  $\beta$  for mongolian gerbil, guinea pig, cat, and squirrel monkey for characteristic frequencies from 0.5–28 kHz.

(4) Each tuning curve is divided into two frequency regions which are separated by an inflection on the lower side of the tip segment at frequency  $f_x$ . For frequencies less than  $f_x$ , the tuning curve is described by the model. For higher frequencies, the threshold tuning curve departs from the model, reaches its BF, and then reaches a high-frequency cutoff.

(5) Inherent to the model is an idealized description of the loss of tuning with raised fiber thresholds that is associated with a simple decrease of the endocochlear potential. For neurons with high values of  $Q_{10\text{dB}}$ , as  $f_x$  increases, the point of departure from the model moves further downward along the curve to lower thresholds. Conversely, neurons with higher thresholds and poorer tuning show adherence to the model for a smaller frequency region. Both  $f_x$  and the BF asymptotically converge along different curves toward the same "limit" or "natural" frequency  $f_n$  as the sensitivity increases (threshold sound levels less than 0 dB).

(6) In terms of recent models of active cochlear function utilizing biological amplification, the higher the "gain," the lower the threshold and the closer  $f_x$  converges toward  $f_n$ . The fiber CF is defined as the value of the BF in the neighborhood of  $f_n$  determined by the normal biological limit on the driving force.

(7) Errors in the fitting of the model to the data are remarkably small and would appear to offer a stronger quali-

ty test than the  $Q_{10\text{dB}}$  for single neuron tuning data. This is because testing for compliance with the model takes into account the local gradient of the frequency-place map and the neural threshold sound level at the frequency of maximum sensitivity.

(8) In its simplest form, the model is appreciated as a spatial constraint upon the origin of the tuning. The relation becomes

$$\Delta x = \alpha p^\beta,$$

where  $\Delta x$  is the distance along the cochlear partition, measured basalward from the *characteristic place* to the place where threshold excitation occurs,  $p$  is the incident sound pressure (Pa),  $\alpha$  is linearly related to the species-dependent gradient of the frequency-place map and  $\beta$  stays close to values of 0.5.

(9) The model may possess a physical interpretation in terms of the motion of the basilar membrane. As such, the model points to a simplification of the description of the shape of the tip segment of the tuning curve. The interpretation is that the tuning arises because the traveling wave sets up an *excitatory region* bordered on each side by regions of inhibition (LePage, 1987b). The model describes the spatial dependence upon sound level of the transition from inhibition to excitation on the basal side of the traveling wave envelope.

(10) The spatial approach may be generalized to other mammals, illustrated by the species adaptation which has occurred for echo location in the horseshoe bat.

*Note added in proof:* Patuzzi *et al.* (1987) have recently shown a strong correlation between the threshold of the neural compound action potential (CAP) to high-frequency tone bursts and the amplitude of the cochlear microphonic to a continuous tone at 200 Hz also obtained from the first turn. The measurement of each were not concurrent. A threshold shift of 37 dB in the CAP corresponds to a 50% reduction (6-dB change) in CM amplitude for a 70-dB SPL tone, while a 54-dB threshold shift corresponds to a 90% reduction (20-dB change). The authors suggest that their data are consistent with the interpretation that temporary hearing loss results from changes to OHC transduction, rather than changes in the electromechanical feedback process.

Their data do suggest that a reduction in the efficiency of outer hair cell transduction may play a role in hearing loss, but they certainly do not rule out the possibility of a much larger influence on the force generation process. Moreover, the results are no less consistent with the idea of a long-term bias of the basilar membrane, causing the temporary threshold loss by modifying the operating points of the inner hair cells and simultaneously having the small effect upon transduction which they show.

The model presented here suggests that it is primarily the force generation process which becomes disabled, and so the biological mechanism needs to be driven harder, i.e., higher stimulus levels, to evoke a baseline shift. Implicit in the model is the suggestion that outer hair cell shape changes are fundamental to inner hair cell transduction at high frequencies. This is why hearing at high frequencies is so criti-

cally dependent on the normal function of the outer hair cells.

## ACKNOWLEDGMENTS

Parts of this work are taken from the Ph.D. thesis by the author. The curve fitting algorithm was implemented by G. K. Yates. I thank B. M. Johnstone for helpful discussions in an early stage of this work, C. E. Molnar for encouragement, and H. Davis for helpful suggestions for refinements to the manuscript. This work was carried out under a post-graduate studentship from the University of Western Australia, NIH Grants NS 07498 and NS 16589 and assistance from Boston University.

<sup>1</sup>This particular set of curves is corrected for the displacement of the stapes, which may make some slight difference to the values of  $\alpha$  and  $\beta$ ; however, it is clear that the model fits the data with equal ease.

- Alder, V. A. (1978). "Neural Correlates of Auditory Temporary Threshold Shift," Ph.D. thesis (Univ. of Western Australia, Nedlands, Australia).
- Allen, J. B. (1983). "Magnitude and phase-frequency response to single tones in the auditory nerve," *J. Acoust. Soc. Am.* **73**, 2071-2092.
- Bruns, V. (1976). "Peripheral auditory tuning for fine frequency analysis by the CF-FM Bat, *Rhinolophus ferrumequinum*. II. Frequency mapping in the cochlea," *J. Comp. Physiol.* **106**, 87-97.
- Bruns, V., and Schmieszek, E. (1980). "Cochlear innervation in the greater horseshoe bat: Demonstration of an acoustic fovea," *Hear. Res.* **3**, 27-43.
- Cody, A. R., and Johnstone, B. M. (1980). "Single auditory neuron response during acute acoustic trauma," *Hear. Res.* **3**, 3-16.
- Dallos, P., and Harris, D. (1978). "Properties of auditory nerve responses in absence of outer hair cells," *J. Neurophysiol.* **41**, 365-383.
- deBoer, E. (1983a). "On active and passive cochlear models—towards a generalized analysis," *J. Acoust. Soc. Am.* **73**, 574-576.
- deBoer, E. (1983b). "Power amplification in an active model of the cochlea—short-wave case," *J. Acoust. Soc. Am.* **73**, 577-579.
- Duifhuis, H., and Vater, M. (1986). "On the mechanics of the horseshoe bat cochlea," in *Peripheral Auditory Mechanisms*, edited by J. B. Allen, J. L. Hall, A. E. Hubbard, S. T. Neely, and A. Tubis (Springer, Berlin, *Lecture Notes in Biomathematics*), Vol. 64, pp. 89-96.
- Evans, E. F. (1974). "Reversible effects of cyanide and furosemide on the tuning of single cochlear nerve fibres," *J. Physiol. (London)* **242**, 129-131.
- Evans, E. F., and Wilson, J. P. (1973). "The frequency selectivity of the cochlea," in *Basic Mechanisms in Hearing*, edited by A. R. Møller (Academic, New York).
- Evans, E. F., and Wilson, J. P. (1975). "Cochlear tuning properties: Concurrent basilar membrane and single nerve fiber measurements," *Science* **190**, 1218-1221.
- Frishkopf, L. S., and deRosier, D. J. (1983). "Mechanical tuning of free-standing stereociliary bundles and frequency analysis in the alligator lizard cochlea," *Hear. Res.* **12**, 393-404.
- Geisler, C. D., Rhode, W. S., and Kennedy, D. T. (1974). "Responses to tonal stimuli of single auditory nerve fibers and their relationship to basilar membrane motion in the squirrel monkey," *J. Neurophysiol.* **37**, 1156-1172.
- Hall, J. L. (1977). "Spatial differentiation as an auditory 'second filter': Assessment on a nonlinear model of the basilar membrane," *J. Acoust. Soc. Am.* **61**, 520-524.
- Huggins, W. H., and Licklider, J. C. R. (1951). "Place mechanisms of auditory frequency analysis," *J. Acoust. Soc. Am.* **23**, 290-299.
- Kiang, N. Y.-S., Liberman, M. C., and Levine, R. A. (1976). "Auditory-nerve activity in cats exposed to ototoxic drugs and high intensity sounds," *Ann. Otol. Rhinol. Laryngol.* **75**, 752-768.
- Kim, D. O., and Molnar, C. E. (1979). "A population study of cochlear nerve fibers: comparison of spatial distributions of average-rate and phase-locking measures of responses to single tones," *J. Neurophysiol.* **42**, 16-30.
- LePage, E. L. (1981). "The role of nonlinear mechanical processes in mammalian hearing," Ph.D. thesis (Univ. of Western Australia, Nedlands, Australia).
- LePage, E. L. (1987a). "Frequency-dependent self-induced bias of the basilar membrane and its potential for controlling sensitivity and tuning in the mammalian cochlea," *J. Acoust. Soc. Am.* **82**, 139-154.
- LePage, E. L. (1987b). "Resonant tuning and spatial filtering in the mammalian cochlea: A paradox or both," in preparation.
- LePage, E. L., and Hubbard, A. E. (1986). "Basilar membrane motion in guinea pig cochlea exhibits frequency-dependent dc offset," in *Peripheral Auditory Mechanisms*, edited by J. B. Allen, J. L. Hall, A. E. Hubbard, S. T. Neely, and A. Tubis (Springer, Berlin, *Lecture Notes in Biomathematics*), Vol. 64, pp. 274-281.
- LePage, E. L., and Johnstone, B. M. (1980). "Nonlinear mechanical behaviour of the basilar membrane in the basal turn of the guinea pig cochlea," *Hear. Res.* **2**, 183-189.
- Liberman, M. C. (1982). "The cochlear frequency map for the cat: Labeling auditory-nerve fibers of known characteristic frequency," *J. Acoust. Soc. Am.* **72**, 1441-1449.
- Liberman, M. C. (1984). "Single neuron labeling and chronic cochlear pathology. I. Threshold shift and characteristic-frequency shift," *Hear. Res.* **16**, 33-41.
- Liberman, M. C., and Dodds, L. W. (1984). "Single-neuron labeling and chronic cochlear pathology. III. Stereocilia damage and alterations of threshold tuning curves," *Hear. Res.* **16**, 55-74.
- Liberman, M. C., and Kiang, N. Y.-S. (1978). "Acoustic trauma in cats. Cochlear pathology and auditory-nerve activity," *Acta Otolaryngol. Suppl.* **358**, 1-63.
- Neely, S. T., and Kim, D. O. (1983). "An active cochlear model showing sharp tuning and high sensitivity," *Hear. Res.* **9**, 123-130.
- Patuzzi, R. B., Yates, G. K., and Johnstone, B. M. (1987). "Noise trauma and outer hair cell impairment," A 24th Workshop on Inner Ear Biology, Nijmegen, The Netherlands, 30 August-2 September 1987.
- Rhode, W. S. (1971). "Observations of the vibration of the basilar membrane in squirrel monkeys using the Mössbauer technique," *J. Acoust. Soc. Am.* **49**, 1218-1231.
- Robertson, D. (1983). "Functional significance of dendritic swelling after loud sounds in the guinea pig cochlea," *Hear. Res.* **9**, 263-278.
- Robertson, D. (1984). "Horseshoe peroxidase injection of physiologically characterised afferent and efferent neurons in the guinea pig spiral ganglion," *Hear. Res.* **15**, 113-121.
- Robertson, D., and Johnstone, B. M. (1979). "Aberrant tonotopic organization in the inner ear damaged by kanamycin," *J. Acoust. Soc. Am.* **66**, 466-469.
- Robertson, D., and Manley, G. A. (1974). "Manipulation of frequency analysis in the cochlear ganglion of the guinea pig," *J. Comp. Physiol.* **91**, 363-378.
- Robertson, D., Cody, A. R., Bredberg, G., and Johnstone, B. M. (1978). "Response properties of spiral ganglion neurons in cochleas damaged by direct mechanical trauma," *J. Acoust. Soc. Am.* **67**, 1295-1303.
- Robertson, D., Cody, A. R., Bredberg, G., and Johnstone, B. M. (1980). "Response properties of spiral ganglion neurons in cochleas damaged by direct mechanical trauma," *J. Acoust. Soc. Am.* **67**, 1295-1303.
- Schmiedt, R. A., Zwislocki, J. J., and Hamernik, R. P. (1980). "Effects of hair-cell lesions on responses of cochlear nerve fibers. I. Lesions, tuning curves, two-tone inhibition and responses to trapezoidal-wave patterns," *J. Neurophysiol.* **43**, 1367-1389.
- Sellick, P. M., Patuzzi, R., and Johnstone, B. M. (1982). "Measurement of basilar membrane motion in the guinea pig cochlea using the Mössbauer technique," *J. Acoust. Soc. Am.* **72**, 131-141.
- Sewell, W. (1984). "The effects of furosemide on the endocochlear potential and auditory-nerve fiber tuning curves in cats," *Hear. Res.* **14**, 305-314.
- Suga, N., Neuweiler, G., and Möller, J. (1976). "Peripheral auditory tuning for fine frequency analysis by the CF-BM Bat, *Rhinolophus ferrumequinum*. IV. Properties of peripheral auditory neurons," *J. Comp. Physiol.* **106**, 111-125.
- Wolberg, J. R. (1967). *Prediction Analysis* (Van Nostrand, Princeton, NJ).